Stochastic Approach to Highway Traffic

R. Mahnke[a], J. Kaupužs[b], I. Lubashevsky[c] and J. Tolmacheva[a,d]

[a] Department of Physics, Rostock University, D–18051 Rostock, Germany
[b] Institute of Mathematics and Computer Science, University of Latvia, LV–1459 Riga, Latvia
[c] General Physics Institute, Russian Academy of Sciences, Moscow, 119991, Russia
[d] Theoretical Physics Department, Institute of Single Crystals, National Academy of Science of Ukraine, 61001 Kharkov, Ukraine

ABSTRACT

We analyze the characteristic features of jam formation on a circular one–lane road. We have applied an optimal velocity model including stochastic noise, where cars are treated as moving and interacting particles. The motion of N cars is described by the system of $2N$ stochastic differential equations with multiplicative white noise. Our system of cars behaves in qualitatively different ways depending on the values of control parameters c (dimensionless density), b (sensitivity parameter characterising the fastness of relaxation), and a (dimensionless noise intensity). In analogy to the gas–liquid phase transition in supersaturated vapour at low enough temperatures, we observe three different regimes of traffic flow at small enough values of $b < b_{cr}$. There is the free flow regime (like gaseous phase) at small densities of cars, the coexistence of a jam and free flow (like liquid and gas) at intermediate densities, and homogeneous dense traffic (like liquid phase) at large densities. The transition from free flow to congested traffic occurs when the homogeneous solution becomes unstable and evolves into the limit cycle. The opposite process takes place at a different density, so that we have a hysteresis effect and phase transition of the first order. A phase transition of second order, characterised by critical exponents, takes place at a certain critical density $c = c_{cr}$. Inclusion of the stochastic noise allows us to calculate the distribution of headway distances and time headways between the successive cars, as well as the distribution of jam (car cluster) sizes in a congested traffic.

Keywords: Traffic flow, Optimal velocity model, Linear stability analysis, Multiplicative noise, Cluster formation, Critical phenomena

1. INTRODUCTION

The aggregation of particles out of an initially homogeneous situation is well known in physics. Depending on the system under consideration and its control parameters the cluster formation in a supersaturated (metastable or unstable) situation has been observed in nucleation physics as well as in other branches.[1] We investigate the well–known example of condensation (formation of liquid droplets) in an undercooled vapour to conclude that the formation of bound states as a phase transition is related to transportation science.

In these terms the breakdown occurs through the formation of a certain critical nucleus in the metastable vehicle flow, which enables us to confine ourselves to a one–cluster–model. We assume that, first, the growth of the car cluster is governed by attachment of cars to the cluster whose rate is mainly determined by the mean headway distance between the car in the vehicle flow and, may be, also by the headway distance in the cluster. Second, the cluster dissolution is determined by the car escape from the cluster whose rate depends on the cluster size directly. The latter is justified using the available experimental data for the correlation properties of the synchronized mode. We write the appropriate master equation,[2–6] converte it into the Fokker–Planck equation for the cluster distribution function and analyze the formation of the critical car cluster due to the climb over a certain potential barrier.[7] The further cluster growth irreversibly gives rise to the jam formation. Numerical estimates of the obtained characteristics and the experimental data of the traffic breakdown are compared.

Further author information: (Send correspondence to Reinhard Mahnke)
E-mail: reinhard.mahnke@physik.uni-rostock.de, Telephone: +49 381 498-6944

2. PHYSICS OF JAM FORMATION IN TRAFFIC FLOW

2.1. Equations of Motion: Deterministic Approach

2.1.1. Introduction. Bando model

Here we investigate the law of motion for circular traffic in terms of headway distances and velocity differences between neighbouring cars. At first, we describe the motion according to the well known Bando model.[8–10] Based on the stationary solution we construct the general solution which can be found from $2N$ differential equations of first oder with respect to time. Using knowledge from matrix theory,[11] we obtain the characteristic equation from which we find Lyapunov exponents of our system.

We consider a model of point–like cars moving on a circular road of length L. The total number of cars is N. We would like to describe the motion of our system. For each car, it is necessary to find its coordinate $x_i(t)$ and velocity $v_i(t)$, for all vehicles $i = 1, \ldots, N$. Within the framework of Bando's model, we have the following law of motion as a system of $2N$ first–oder differential equations for the unknown functions $v_i(t)$ and $x_i(t)$ with respect to time t

$$\frac{dv_i}{dt} = \frac{1}{\tau}\left(v_{opt}(\Delta x_i) - v_i\right) ; \tag{1}$$

$$\frac{dx_i}{dt} = v_i \tag{2}$$

where $v_{opt}(\Delta x)$ is the optimal velocity function given by the following expression

$$v_{opt}(\Delta x) = v_{max}\,\frac{(\Delta x)^2}{D^2 + (\Delta x)^2} \tag{3}$$

where $\Delta x_i = x_{i+1} - x_i$ is the headway (bumper-to-bumper distance), v_{max} is the maximal speed allowed and D is a given positive control parameter called interaction distance. According to the periodic boundary condition we find

$$\sum_{i=1}^{N} \Delta x_i = 0 \, . \tag{4}$$

We would like to introduce new dimensionless variables for velocities, coordinates and time in the following way

$$u_i = v_i / v_{max} \, , \quad y_i = x_i / D \, , \quad T = t/\tau \, . \tag{5}$$

After transformation (5) the dynamical system (1) – (2) can be rewritten as

$$\frac{du_i}{dT} = u_{opt}(\Delta y_i) - u_i \, ; \tag{6}$$

$$\frac{dy_i}{dT} = \frac{1}{b}\,u_i \, , \tag{7}$$

where the dimensionless optimal velocity u_{opt} and the dimensionless control parameter b are given as

$$u_{opt}(\Delta y) = \frac{(\Delta y)^2}{1 + (\Delta y)^2} \qquad \text{and} \qquad b = \frac{D}{\tau\, v_{max}} \, . \tag{8}$$

2.1.2. Neighbouring cars. Stationary solution

It is interesting to consider the system of equations (6) – (7) in terms of headway distances and velocity differences between the neighbouring cars. For this purpose, we take the difference between the $(i+1)$–th and the i–th equation, which yields

$$\frac{d(u_{i+1} - u_i)}{dT} = \left(u_{opt}(\Delta y_{i+1}) - u_{opt}(\Delta y_i)\right) - (u_{i+1} - u_i) \, , \tag{9}$$

$$\frac{d(y_{i+1} - y_i)}{dT} = \frac{1}{b}\,(u_{i+1} - u_i) \, , \qquad i = 1, \ldots, N \, . \tag{10}$$

It is naturally to introduce new variables

$$\Delta u_i = u_{i+1} - u_i \qquad ; \qquad \Delta y_i = y_{i+1} - y_i \tag{11}$$

and rewrite (9) – (10) in terms of Δu_i and Δy_i

$$\frac{d(\Delta u_i)}{dT} = (u_{opt}(\Delta y_{i+1}) - u_{opt}(\Delta y_i)) - \Delta u_i) \; ; \tag{12}$$

$$\frac{d(\Delta y_i)}{dT} = \frac{1}{b}\,\Delta u_i, \qquad i = 1, \ldots, N \; . \tag{13}$$

Due to periodic boundary conditions we will have

$$y_{N+1} = y_1 \; . \tag{14}$$

Let us find the stationary solution of the system (12) – (13). It means that functions Δu_i and Δy_i in these equations do not depend on time T. Namely

$$u_{opt}(\Delta y_{i+1}) - u_{opt}(\Delta y_i) - \Delta u_i = 0 \; ; \tag{15}$$

$$\frac{1}{b}\,\Delta u_i = 0 \; . \tag{16}$$

The steady state or free flow solution for all vehicles $i = 1 \ldots N$ is

$$\Delta u_i^{st} = 0 \qquad ; \qquad \Delta y_i^{st} = \frac{\mathcal{L}}{N} \; , \tag{17}$$

where $\mathcal{L} = L/D$ is the dimensionless length of the road.

2.1.3. Lyapunov exponents. Stability analysis

The stability of the stationary solution can be investigated by the method of small perturbations. Let us denote $\delta\Delta u_i$ and $\delta\Delta y_i$ as velocity and coordinate perturbations respectively. Then we obtain

$$\Delta u_i = \Delta u_i^{st} + \delta\Delta u_i \; ; \tag{18}$$

$$\Delta y_i = \Delta y_i^{st} + \delta\Delta y_i \; . \tag{19}$$

Putting these expressions into (12) – (13) we obtain a system of equations in terms of $\delta\Delta u_i$ and $\delta\Delta y_i$

$$\frac{d\,\delta\Delta u_i}{dT} = k\,(\delta\Delta y_{i+1} - \delta\Delta y_i) - \delta\Delta u_i \; , \tag{20}$$

$$\frac{d\,\delta\Delta y_i}{dT} = \frac{1}{b}\delta\Delta u_i \tag{21}$$

where $k = u'_{opt}(\Delta y^{st})$ is the first derivative of the optimal velocity function at the steady state solution.

Let us introduce vector $\vec{x} \in \mathbb{R}^{2N}$

$$\vec{x} = (\delta\Delta y_1, \delta\Delta y_2, ..., \delta\Delta y_N, \delta\Delta u_1, \delta\Delta u_2, ..., \delta\Delta u_N)^T \; . \tag{22}$$

Hence we can write the system of equations (20) – (21) in vector form

$$\dot{\vec{x}} = \mathcal{A}\,\vec{x} \tag{23}$$

where $\mathcal{A}$ is a block matrix with the following structure

$$\mathcal{A} = \begin{bmatrix} \mathcal{O} & \mathcal{B} \\ \mathcal{K} & \mathcal{I} \end{bmatrix} \tag{24}$$

where

$$\mathcal{O} = \begin{bmatrix} 0 & 0 & . & . & 0 & 0 \\ 0 & 0 & . & . & 0 & 0 \\ . & . & . & . & . & . \\ . & . & . & . & . & . \\ 0 & 0 & . & . & 0 & 0 \\ 0 & 0 & . & . & 0 & 0 \end{bmatrix} ; \qquad \mathcal{B} = \begin{bmatrix} 1/b & 0 & . & . & 0 & 0 \\ 0 & 1/b & . & . & 0 & 0 \\ . & . & . & . & . & . \\ . & . & . & . & . & . \\ 0 & 0 & . & . & 1/b & 0 \\ 0 & 0 & . & . & 0 & 1/b \end{bmatrix} , \tag{25}$$

$$\mathcal{K} = \begin{bmatrix} -k & k & . & . & 0 & 0 \\ 0 & -k & . & . & 0 & 0 \\ . & . & . & . & . & . \\ . & . & . & . & . & . \\ 0 & 0 & . & . & -k & k \\ k & 0 & . & . & 0 & -k \end{bmatrix} , \qquad \mathcal{I} = \begin{bmatrix} -1 & 0 & . & . & 0 & 0 \\ 0 & -1 & . & . & 0 & 0 \\ . & . & . & . & . & . \\ . & . & . & . & . & . \\ 0 & 0 & . & . & -1 & 0 \\ 0 & 0 & . & . & 0 & -1 \end{bmatrix} . \tag{26}$$

It is necessary to find the eigenvalues of matrix $\mathcal{A}$ for solving the vector differential equation (23). For this purpose we construct the characteristic polynomial of matrix $\mathcal{A}$ (see Ref. 11)

$$\mathcal{P}(\lambda) = \det(\mathcal{A} - \lambda\mathcal{E}_{2N\times 2N}) = \det \begin{bmatrix} \mathcal{O} - \lambda\mathcal{E}_{N\times N} & \mathcal{B} \\ \mathcal{K} & \mathcal{I} - \lambda\mathcal{E}_{N\times N} \end{bmatrix} = \det \begin{bmatrix} \Lambda & \mathcal{B} \\ \mathcal{K} & \mathcal{Y} \end{bmatrix} \tag{27}$$

where $\mathcal{E}_{2N\times 2N}$ and $\mathcal{E}_{N\times N}$ are identity matrices with dimension $2N \times 2N$ and $N \times N$ respectively. Matrices Λ and $\mathcal{Y}$ are given by

$$\Lambda = \begin{bmatrix} -\lambda & 0 & . & . & 0 & 0 \\ 0 & -\lambda & . & . & 0 & 0 \\ . & . & . & . & . & . \\ . & . & . & . & . & . \\ 0 & 0 & . & . & -\lambda & 0 \\ 0 & 0 & . & . & 0 & -\lambda \end{bmatrix} , \tag{28}$$

$$\mathcal{Y} = \begin{bmatrix} -1-\lambda & 0 & . & . & 0 & 0 \\ 0 & -1-\lambda & . & . & 0 & 0 \\ . & . & . & . & . & . \\ . & . & . & . & . & . \\ 0 & 0 & . & . & -1-\lambda & 0 \\ 0 & 0 & . & . & 0 & -1-\lambda \end{bmatrix} . \tag{29}$$

The eigenvalues are the solutions of the equation

$$\mathcal{P}(\lambda) = 0 . \tag{30}$$

As a trivial solution, one eigenvalue is $\lambda = -1$. Since $\det \mathcal{Y} \neq 0$ holds for other eigenvalues ($\lambda \neq -1$), the calculation of determinant (27) can be simplified[11]

$$\det \begin{bmatrix} \Lambda & \mathcal{B} \\ \mathcal{K} & \mathcal{Y} \end{bmatrix} = \det \begin{bmatrix} \Lambda - \mathcal{B}\mathcal{Y}^{-1}\mathcal{K} & 0 \\ \mathcal{K} & \mathcal{Y} \end{bmatrix} = \det\left(\Lambda - \mathcal{B}\,\mathcal{Y}^{-1}\mathcal{K}\right)\det\left(\mathcal{Y}\right) . \tag{31}$$

Hence, the characteristic polynomial has the form

$$\mathcal{P}(\lambda) = (-1-\lambda)^N \det\left(\Lambda - \mathcal{B}\mathcal{Y}^{-1}\mathcal{K}\right) = \left((-1-\lambda) + \frac{k}{b}\right)^N - \left(\frac{k}{b}\right)^N \tag{32}$$

and all eigenvalues λ_i, $i = 1, \ldots, 2N$ are found from equation (32) using (30). Since k/b is a nonzero constant the characteristic equation $\mathcal{P}(\lambda) = 0$ can be rewritten as

$$\left(\frac{b}{k}\left(-1-\lambda\right) + 1\right)^N - 1 = 0 . \tag{33}$$

Using the fact that $\sqrt[N]{1} = \exp\left(\frac{2\pi m}{N}\right) = \cos\left(\frac{2\pi m}{N}\right) + i\sin\left(\frac{2\pi m}{N}\right)$, $m = 0, \ldots, N-1$ we obtain the following quadratic equation

$$\lambda^2 + \lambda + \frac{k}{b}\left(1 - \exp\left(\frac{2\pi m}{N}\right)\right) = 0 \tag{34}$$

which can be solved easily by putting $\lambda = \mathrm{Re}\,\lambda + i\,\mathrm{Im}\,\lambda = \alpha + i\beta$. Hence, α and β are solutions of the system

$$\alpha^2 - \beta^2 + \alpha + \frac{k}{b}\left(1 - \cos\left(\frac{2\pi m}{N}\right)\right) = 0\,, \tag{35}$$

$$2\alpha\,\beta + \beta - \frac{k}{b}\,\sin\left(\frac{2\pi m}{N}\right) = 0\,. \tag{36}$$

The homogeneous solution looses the stability at a certain value of k/b when α vanishes for some m. According to (35) – (36), it takes place at

$$\alpha = 0\,, \quad \beta = \frac{k}{b}\,\sin\left(\frac{2\pi m}{N}\right)\,, \quad \frac{k}{b} = \frac{1}{1 + \cos\left(\frac{2\pi m}{N}\right)}\,. \tag{37}$$

The stability border corresponds to the value of k/b at which the real part of one of the eigenvalues vanishes for the first time and then becomes positive if k/b is increased. It occurs first with the eigenvalue indexed by $m = 1$, since for $m = 0$ we have got $\lambda = 0 \equiv \lambda_0$ and $\lambda \equiv -1$.

Let us find the eigenvector $\vec{x}_0$ which correponds to λ_0. It is given by

$$\mathcal{A}\,\vec{x}_0 = \lambda_0\,\vec{x}_0\,. \tag{38}$$

According to that fact that matrix $\mathcal{A}$ has the block structure (24) we define vector $\vec{x}_0$ as two component vector

$$\vec{x}_0 = \begin{bmatrix} \vec{x}_0^{\,1} \\ \vec{x}_0^{\,2} \end{bmatrix} \tag{39}$$

where $\vec{x}_0^{\,1}$ and $\vec{x}_0^{\,2}$ are N-dimensional vectors. Then the vector equation can be written

$$\begin{bmatrix} \mathcal{O} & \mathcal{B} \\ \mathcal{K} & \mathcal{I} \end{bmatrix} \begin{bmatrix} \vec{x}_0^{\,1} \\ \vec{x}_0^{\,2} \end{bmatrix} = \lambda_0 \begin{bmatrix} \vec{x}_0^{\,1} \\ \vec{x}_0^{\,2} \end{bmatrix}\,. \tag{40}$$

The linear system respect to vectors $\vec{x}_0^{\,1}$ and $\vec{x}_0^{\,2}$ is followed by the equation (40)

$$\mathcal{B}\,\vec{x}_0^{\,2} = \lambda_0\,\vec{x}_0^{\,1} \tag{41}$$

$$\mathcal{K}\,\vec{x}_0^{\,1} + \mathcal{I}\,\vec{x}_0^{\,2} = \lambda_0\,\vec{x}_0^{\,2}\,. \tag{42}$$

Due to the fact that right parts of vector equations (41) – (42) equal to zero, i. e. $\lambda_0 = 0$, we obtain that vectors $\vec{x}_0^{\,1}$ and $\vec{x}_0^{\,2}$ are linearly independent. That is why, we can say that vector $\vec{x}_0^{\,1}$ equals to one (it means, according to construction of $\vec{x}_0^{\,1}$ and $\vec{x}_0^{\,2}$, that each component of $\vec{x}_0^{\,1}$ is equal to one) and vector $\vec{x}_0^{\,2}$ can be found using (26) and (41) – (42). Namely,

$$\mathcal{K}\,\vec{x}_0^{\,1} = -\,\mathcal{I}\,\vec{x}_0^{\,2} \tag{43}$$

or in other words, component by

$$\begin{bmatrix} -k + k \\ k + (-k) \\ . \\ . \\ k + (-k) \end{bmatrix} = \begin{bmatrix} -x_{0,1}^2 \\ -x_{0,2}^2 \\ . \\ . \\ -x_{0,N}^2 \end{bmatrix}\,. \tag{44}$$

We obtain that each component of $\vec{x}_0^{\,2}$ equals to zero. As result, we can write the eigenvector $\vec{x}_0$ which corresponds to zero eigenvalue λ_0. We find

$$\vec{x}_0 = [\underbrace{1\,,\,1\,,\,..1\,,1}_{N},\underbrace{0\,,\,0\,,\,..0\,,\,0}_{N}]^T\,. \tag{45}$$

The another interesting fact, that decomposition coefficient c_0 of any vector $\vec{x}$ (22) on eigenvalue λ_0 and eigenvector $\vec{x}_0$ is equal to zero. It is easy to see, that is

$$c_0 = \vec{x} \cdot \vec{x}_0 = \sum_{i=1}^{N} x_i = \sum_{i=1}^{N} \delta \Delta y_i = 0 \tag{46}$$

in connection with periodic boundary condition (4). The operator $\cdot$ means the scalar product of two vectors in $\mathbb{R}^{2N}$.

2.1.4. Stability diagram

We are interested in studying the stability regions in b-c-plane, where $c = N/\mathcal{L}$ is the dimensionless density of cars, both for homogeneous and heterogeneous solutions depending on the initial conditions as well as the total number of cars N. The homogeneous flow described by the stationary solution of (6) – (7), i. e., $\Delta y_i^{st} = \mathcal{L}/N = 1/c$ and $u_i^{st} = u_{opt}\,(\Delta y_i^{st})$, becomes unstable when entering the region $b < b(c)$, where $b(c)$ is given by

$$b(c) = u'_{opt}\left(\frac{1}{c}\right)\,\left(1 + \cos\left(\frac{2\pi}{N}\right)\right) \tag{47}$$

with

$$u'_{opt}\left(\frac{1}{c}\right) = \frac{2\,c^3}{(1+c^2)^2}\ , \tag{48}$$

as consistent with the stability condition (37) at $m = 1$. The maximum of $b(c)$ corresponds to the critical concentration $c_{cr} = \sqrt{3}$. The finite–size effect on the phase diagram, where the regions of stable and unstable homogeneous flow are separated by $b(c)$ curve, is illustrated in Fig. 1. The homogeneous stationary solution (12)–

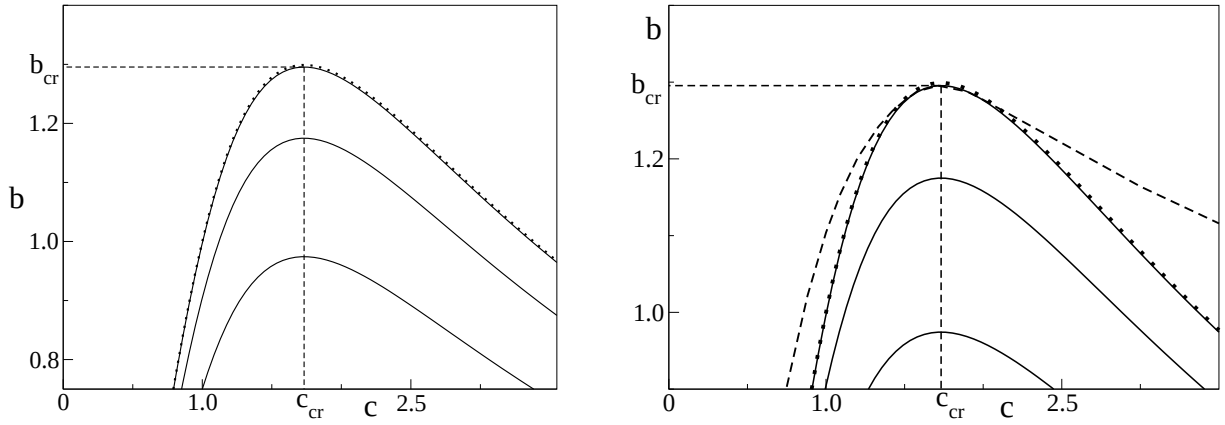

Figure 1. Phase diagram as b-c-plane for a system with fixed different number of cars N. From the bottom to the top solid curves $b(c)$ show the stability border of the homogeneous traffic flow at $N = 6$, $N = 10$, and $N = 60$, respectively. The dotted curve is the function $b(c)$ when N tends to infinity. Each $b(c)$ plot has a maximum at the critical density $c_{cr} = \sqrt{3} \approx 1.732$. The maximum value at $N \to \infty$ is $b_{cr} = 3\sqrt{3}/4 \approx 1.299$. The dashed curve in the right hand side figure shows the stability border of the heterogeneous traffic flow at $N = 60$ (numerical simulation). It becomes unstable when exiting the region below this curve.

(13) transforms into a heterogeneous limit–cycle solution when entering the region below the $b(c)$ curve. The stability of the limit–cycle solution for $N = 60$ cars has been studied numerically, and we have found that it becomes unstable when exiting the region below the dashed curve shown in Fig. 1 (right). In other words, like in many physical systems (e. g. supersaturated vapour), we observe a hysteresis effect which is a property of the first–order phase transition. The stationary state of the system between the solid and dashed curves (at a given N) is of the same type as the initial conditions.

2.1.5. Bifurcation diagrams and critical exponents

According to the stability diagram discussed in Sec. 2.1.4, a phase transition from heterogeneous state to homogeneous one takes place at a fixed density c when parameter b is increased and reaches the dashed curve in Fig. 1 (right). The heterogeneous state is characterised by the minimal u_{min} and the maximal u_{max} values of the velocity u in the limit cycle. At the critical density $c = c_{cr} = \sqrt{3}$ both branches $u_{min} = u_{min}(b)$ and $u_{max} = u_{max}(b)$ continuously mearge into one branche $u_{min}(b) = u_{max}(b) = u_{hom}$ at the critical point $b = b_{cr} = (3\sqrt{3}/8)(1 + \cos(2\pi/N))$, where $u_{hom} = 1/(1 + c^2)$ is the steady state velocity of the homogeneous flow. It is the supercritical bifurcation diagram shown in Fig. 2 (right) for a finite number of cars $N = 60$. The transformation is discontinuous at $c \neq c_{cr}$, as consistent with the subcritical bifurcation diagram at $c = 1.5$ on the left hand side of Fig. 2. These diagrams have been considered earlier.[12] Now we have made a more precise

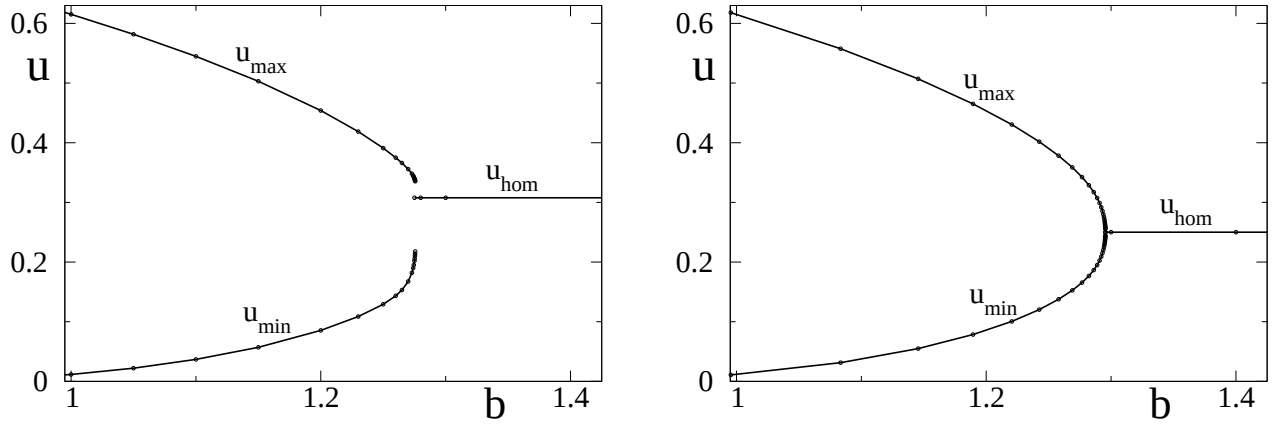

Figure 2. Subcritical bifurcation diagram at $c = 1.5$ (left) and supercritical bifurcation diagram at the critical density $c = c_{cr} = \sqrt{3}$ (right) for the minimal and maximal velocities depending on the control parameter b at a fixed number of cars $N = 60$.

calculation by using the analytically determined exact values of c_{cr} and b_{cr} to evaluate more precisely the critical exponents β_1 and β_2, which are related to the power–like singularities of u_{max} and u_{min} at $c = c_{cr}$ and $b \to b_{cr}$, i. e.,

$$u_{max}(b) - u_{hom} \propto (b_{cr} - b)^{\beta_1} \tag{49}$$

$$u_{hom} - u_{min}(b) \propto (b_{cr} - b)^{\beta_1} \ . \tag{50}$$

We have defined the effective critical exponents $\beta_1^{eff}(h)$ and $\beta_2^{eff}(h)$ as the slope of the log–log plot evaluated from the data at $b = b_{cr} - h$ and $b = b_{cr} - 2h$. The results are shown in Fig. 3. The true (asymptotic) values of the critical exponents are obtained at $h \to 0$. Fig. 3 represents a numerical evidence that both exponents β_1 and β_2 have the same universal mean–field value $1/2$. It shows also that an evaluation of critical exponent by simply measuring the slope of the log-log plot at a quite small distance from the critical point, e. g. at $h \sim 0.006$, is rather misleading.

2.1.6. Advanced Bando model

A disadvantage of the optimal velocity model (1)–(2) is that it is not collision free. In other words, it does not ensure the solution where all the headway distances are always positive. In particular, we never succeded to get a limit–cycle solution without collisions at $b < 0.86$. An important feature of Bando as well as our optimal velocity model (1)–(2) is the symmetry between acceleration and braking. In real traffic, however, the braking (deceleration) can be remarkably larger than the acceleration, which is important to avoid collisions. Below we propose a collision–free model which includes this asymmetry.

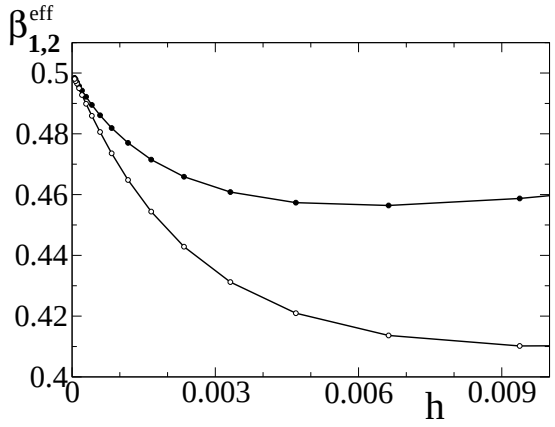

Figure 3. The effective critical exponets $\beta_1^{eff}(h)$ (solid circles) and $\beta_2^{eff}(h)$ (empty circles) estimated from the $u_{max}(b)$ and $u_{min}(b)$ data, respectively, at finite distances from the critical point: $b = b_{cr} - h$ and $b = b_{cr} - 2h$. The universal asymptotic value of the critical exponent $\beta = 0.5$ is obtained at $h \to 0$.

According to Newton law of motion and using our old notations we have the following set of $2N$ differential equations

$$m\frac{dv_i}{dt} = F_{det}(v_i, \Delta x_i)\ ; \tag{51}$$

$$\frac{dx_i}{dt} = v_i \tag{52}$$

where m is mass of point-like particle. Now we split the deterministic force $F_{det}(v_i, \Delta x_i)$ into two parts

$$F_{det}(v_i, \Delta x_i) = F_{acc}(v_i) + F_{dec}(v_i, \Delta x_i) \tag{53}$$

with acceleration and deceleration ansatz

$$F_{acc}(v_i) = \frac{m}{\tau}\,(v_{max} - v_i) \geq 0 \tag{54}$$

$$F_{dec}(v_i, \Delta x_i) = \frac{m}{\tau}\,(v_{opt}(\Delta x_i) - v_{max})\left(1 + \left(p\frac{v_i}{\Delta x_i}\right)^2\right) \leq 0 \tag{55}$$

taking into account the optimal velocity function (3). The deceleration force F_{dec} includes a symmetry–breaking term with new parameter p. A simple consideration shows that a deceleration $-dv_i/dt > v_0^2/(2\Delta x)$ is large enough for a car moving with initial velocity v_0 to stop before a vehicle staying in front of it at an initial distance Δx. According to safety considerations, a car has to decelerate even stronger at small distances Δx, therefore we have assumed in (55) that the additional term in F_{dec} is proportional to $(v_i/\Delta x_i)^2$. At this condition a car never can reach with nonzero velocity $v' = v_i(t')$ (at a time moment $t = t'$) another car staying in front of it, since the assumption $v' > 0$ leads to a contradiction: it implies that $-dv_i/dt > v_i^2(t_0)/(2\Delta x(t_0))$ holds within certain time interval $t_0 < t < t'$, which by itself rules out the collision. The original Bando model (1)–(2) is recovered at $p = 0$. If p is a small parameter, then the new model behaves practically in the same way as the old one, except only those critical situations where some car produces an accident in the old model, and now its motion is corrected to avoid the collision. The deceleration force term due to to interaction between cars is always negative

$$F_{dec} = -\,v_{max}\frac{m}{\tau}\,\frac{1}{1 + (\Delta x_i/D)^2}\left(1 + \left(p\frac{v_i}{\Delta x_i}\right)^2\right)\ . \tag{56}$$

Using acceleration (54) and deceleration (56) ansatz we are able to write the deterministic force F_{det} as

$$F_{det}(v_i, \Delta x_i) = v_{max}\,\frac{m}{\tau}\left(1 - \frac{v_i}{v_{max}} - \frac{1}{1+(\Delta x_i/D)^2}\right)\left(1 + \left(p\frac{v_i}{\Delta x_i}\right)^2\right). \tag{57}$$

As earlier, it is convenient to make our equations of motion dimensionless (5). Finally we obtain

$$\frac{du_i}{dT} = 1 - u_i - \frac{1}{1+(\Delta y_i)^2}\left(1 + \left(\tilde{p}\frac{u_i}{\Delta y_i}\right)^2\right) \tag{58}$$

$$\frac{dy_i}{dT} = \frac{1}{b}u_i \tag{59}$$

where $\tilde{p} = pv_{max}/D$.

To illustrate the difference between the new and old models, we have made a numerical calculation at $b = 1$ for one car with the initial coordinate $y = 0$ and velocity $u = 0.7$ having a wall (or, equally, another staying car) in front of it at the position $y = 1$. We have plotted in Fig. 4 the velocity u depending on the coordinate y for the Bando model with $\tilde{p} = 0$ (dot–dashed curve), as well as for the new advanced model with $\tilde{p} = 0.2$ (solid curve). As it is seen, the car reaches the wall with nonzero velocity in the original model. To the contrary, no accident occurs in the new model. In this case the car approaches the wall asymptotically at $T \to \infty$ with vanishing velocity $u \to 0$.

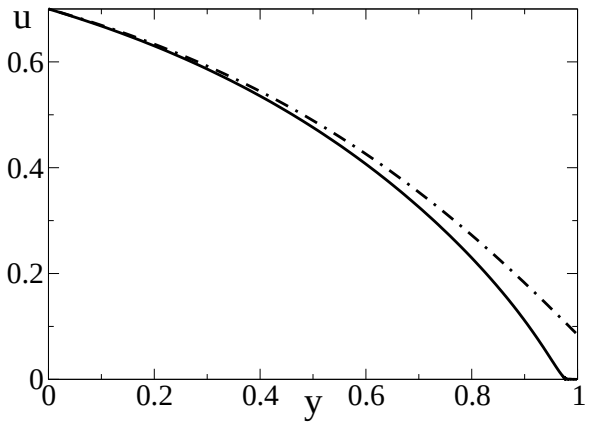

Figure 4. The dimensionless velocity u vs coordinate y for one car with the initial coordinate $y = 0$ and velocity $u = 0.7$ having a wall at the position $y = 1$ in front of it. The dashed line, showing a collision with the wall, corresponds to the optimal velocity model ($\tilde{p} = 0$), whereas the solid line corresponds to the advanced collision–free model with $\tilde{p} = 0.2$.

The homogeneous steady state solution $du_i/dT = 0$ of system (58) – (59) reads

$$1 - u_i - \frac{1}{1+(\Delta y_i)^2}\left(1 + \left(\tilde{p}\frac{u_i}{\Delta y_i}\right)^2\right) = 0\,. \tag{60}$$

It corresponds to equal headways $\Delta y_i = \mathcal{L}/N = 1/c$. The steady state velocity can be found as the positive root of the quadratic equation

$$u_i^2 + \frac{(\Delta y_i)^2}{\tilde{p}^2}\left(1 + (\Delta y_i)^2\right)u_i - \frac{(\Delta y_i)^4}{\tilde{p}^2} = 0 \tag{61}$$

which follows from (60). It yields

$$u_i = \frac{(\Delta y_i)^2(1+(\Delta y_i)^2)}{2\,\tilde{p}^2}\left(\sqrt{1 + \frac{4\,\tilde{p}^2}{(1+(\Delta y_i)^2)^2}} - 1\right). \tag{62}$$

The result of the optimal velocity model $u_i = u_{opt}(\Delta y_i)$ is recovered at $\tilde{p} \to 0$.

In Fig 5 the steady state velocity of the new model with $\tilde{p} = 1$ is compared to that of the optimal velocity model with $\tilde{p} = 0$. The difference is relatively small at $\tilde{p} = 1$ and even much (about 100 times) smaller at $\tilde{p} = 0.1$. The latter implies that the additional term with $\tilde{p}$ practically does not change the properties of the original optimal velocity model at $\tilde{p} \sim 0.1$, except that it makes the model collision free.

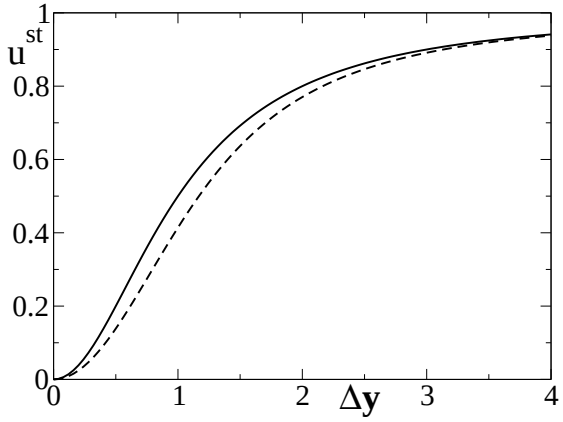

Figure 5. The steady state velocity of a homogeneous traffic flow depending on the headway distance Δy. The solid line corresponds to the optimal velocity model ($\tilde{p} = 0$), the dashed line indicates the result of the new model with $\tilde{p} = 1$.

2.2. Equations of Motion: Langevin Approach

Recently, the theoretical and empirical foundations of *physics of traffic flow* have come into the focus of the physical community, see e. g. Ref. 13. Different approaches like deterministic and stochastic nonlinear dynamics as well as statistical physics of many–particle systems have been very successful in understanding empirically observed structure formation on roads like jam formation in freeway traffic. The motion of an individual vehicle has many peculiarities, since it is controlled by motivated driver behaviour together with physical constraints. Nevertheless, on macroscopic scales the car ensemble displays phenomena like phase formation (nucleation), widely met in different physical systems. Although the cooperative behaviour of cars treated as active particles seems to be more general, we concentrate as before on a well–investigated approximation known as safety distance or optimal velocity (OV) model, first proposed by Bando et al.[8–10]

The OV model of a one-lane road with periodic boundary conditions is based in the Langevin approach on the following set of acceleration equations

$$\frac{dv_i}{dt} = \frac{v_{opt}(\Delta x_i) - v_i}{\tau} + \xi_i(t) \; . \tag{63}$$

Neglecting the noise term ξ_i, the position $x_i(t)$ as well as the velocity $v_i(t)$ of each car $i = 1, \ldots, N$ at every time moment t can be calculated out of the initial values by integrating the coupled equations of motion (remember Sect. 2.1). The coupling is due to the interaction between two successive cars measured by the headway $\Delta x_i = x_{i+1} - x_i - \ell$ (put car length $\ell \to 0$ for point-like cars). The optimal or desired velocity $v_{opt}(\Delta x)$ (3) is the steady–state velocity chosen by drivers as function of the headway between cars. It increases monotoneously with the distance and tends to a constant maximal value v_{max} for $\Delta x \to \infty$.

Our equations of motion can be written as random dynamical system with multiplicative Gaussian white noise[6]

$$m\, dv_i(t) = F_{det}(v_i, \Delta x_i)\, dt + \sigma\, v_i\, dW_i(t) \tag{64}$$

$$dx_i(t) = v_i\, dt \tag{65}$$

for a point–like particle (vehicle i) of mass m with speed $v_i(t)$ at location $x_i(t)$. Here $F_{det} = m\,(v_{opt}(\Delta x_i) - v_i)/\tau$ is the deterministic force. The fluctuations $dW_i = Z\sqrt{dt}$ are given by the increment of a Wiener process, where Z is a $\mathcal{N}(0,1)$ standard normal-distributed random number. By using the dimensionless variables introduced in (5), the system of equations (64)–(65) becomes

$$du_i(t) = (u_{opt}(\Delta y_i) - u_i)\,dT + a\,u_i\,dW_i(t) \tag{66}$$

$$dy_i(t) = \frac{1}{b} u_i\,dT\ , \tag{67}$$

where $a = \sigma\sqrt{\tau}/m$ is the dimensionless noise amplitude.

We have solved numerically (simulated) the system of Eqs. (66)–(67) for a finite system of 60 cars at nonvanishing noise intensity $a = 0.1$ by an algorithm called explicit 1.5 order strong scheme.[14] We have fixed the dimensionless density of cars c and have varied the parameter b to estimate the value $b(c)$ at which the transition from free–flow regime to congested traffic occurs. A jump–like increase in the variance of the velocity $var(u) = \langle u^2\rangle - \langle u\rangle^2$ takes place around $b = b(c)$. The noise tends to wash out the phase transition in finite system we considered, therefore we could not observe a real jump and the value of $b(c)$ has been identified with the inflection point of the $var(u)$ vs b plot where this curve has the maximal steepness. Moreover, the phase transition around the critical density $c_{cr} = \sqrt{3}$ becomes too diffuse to identify the location of the transition point. Due to the fluctuations at $a > 0$, our system of cars cannot stay unlimitedly long time in a metastable state. It means that a sufficiently long simulation will give us one line $b = b(c)$ irrespective to the initial conditions rather than two branches of the phase diagram shown in Fig. 1 (right) for the deterministic case $a = 0$. Nevertheless, even at positive $a = 0.1$ a hysteresis effect has been observed in finite–time sumulations at certain densities, e. g., $c = 3$. The phase diagram in Fig. 6 shows the pieces of $b = b(c)$ curve (dotted line) at $a = 0.1$ as well as the two branches with $a = 0$ for comparison.

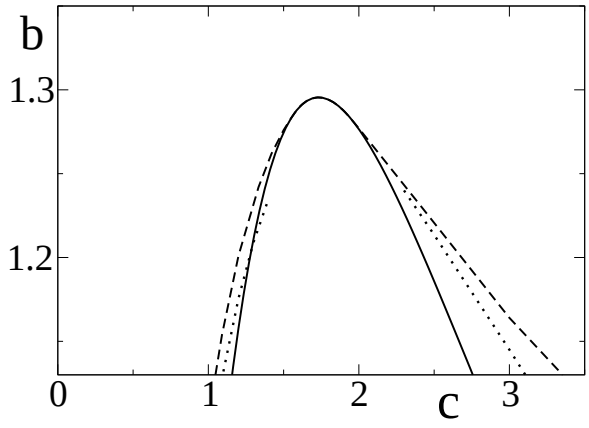

Figure 6. The phase diagram of finite system of $N = 60$ cars, including the phase transition line (dotted curve) at a nonvanishing noise intensity $a = 0.1$. The solid and dashed lines refers to the case $a = 0$ and have the same meaning as in Fig. 1.

The idea to use the variance of the velocity u to distinguish between the homogeneous and heterogeneous states of the system is similar to that applied in Ref. 15, where a closely related quantity, namely, the variance of the density has been considered in framework of stochastic car following models. Particularly, we expect that the stochastic Bando model considered here would produce a similar variance plot depending on the density and noise intensity as does the cellular outomata model dicussed in Ref. 15. The noise, however, can produce collisions in the model (64) – (65), and they become highly probable at large noise intensities. A modification of the deterministic part, as proposed in Sec. 2.1.6, is helpful to solve this problem.

We have fixed the noise intensity $a = 0.1$ and the number of cars $N = 60$ and have studied the distribution of vehicular velocities and headway distances depending on the dimensionless car density c and parameter b. In

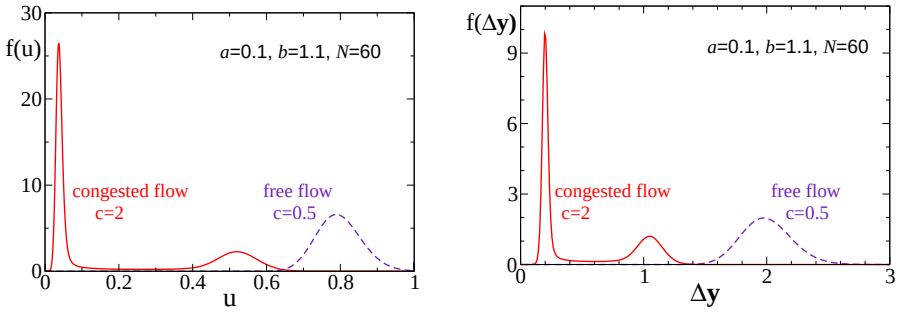

Figure 7. The probability density distribution of velocities (left) and headway distances (right) for two different car densities $c = 0.5$ and $c = 2$ at fixed dimensionless noise amplitude $a = 0.1$ and parameter $b = 1.1$.

Fig. 7 (left) the velocity distribution function $f(u)$ is shown at $b = 1.1$ for a relatively small density $c = 0.5$ as well as for higher density $c = 2$. In the first case we have only one maximum located near $u = 0.8$ which is the steady state velocity of the homogeneous free traffic flow without noise. The noise only smears out the delta–like distribution to yield a smooth maximum seen in Fig. 7. The traffic flow is homogeneous with small fluctuations in velocities and also headway distances, as shown in Fig. 7 (right). The headway–distance distribution function $f(\Delta y)$ has a maximum near $\Delta y = \Delta y_{hom} = 1/c = 2$ which is the average headway distance in a homogeneous flow. In the second case ($c = 2$) the velocity distribution function as well as the headway distribution function have two maxima. It indicates the coexistence of two phases – free flow with relatively large headways and velocities and jam with small headways and velocities.

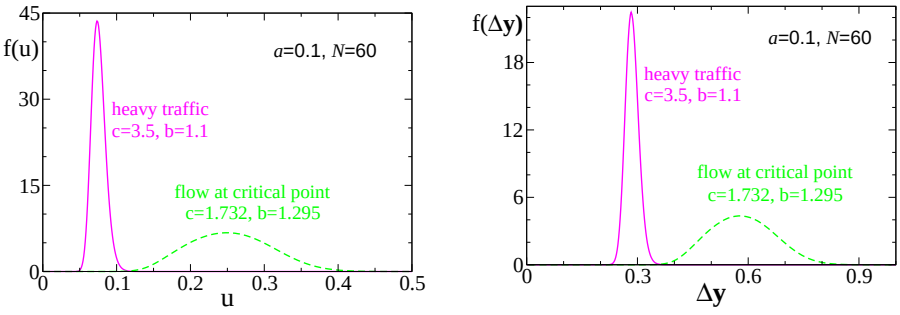

Figure 8. The probability density distribution of velocities (left) and headway distances (right) in the case of heavy traffic with large density of cars $c = 3.5$ (at $b = 1.1$) and at the critical point $c = c_{cr} = \sqrt{3} \simeq 1.73205$, $b = b_{cr} \simeq 1.29548$. In both cases the dimensionless noise intensity is $a = 0.1$.

The heavy traffic at $c = 3.5$, as well as the critical situation at $c = c_{cr}$ and $b = b_{cr}$ are illustrated in Fig. 8 with the same notation as in Fig. 7. In both cases the distributions have only one maximum, as consistent with the existence of only one phase. A distinguishing feature of the critical point is that the distributions over the headway distances and velocities are relatively broad.

The simulation of the stochastic equations (64) and (65) in the coexistence region allows us also to find the probability $P(n, t)$ that just n cars are involved in the jam. In this case the jammed cars are defined as those vehicles which have the headway distance smaller than the homogeneous one $\Delta y_{hom} = 1/c$. The results of numerical simulation at $c = 2$ coincide qualitatively with the investigations of the stochastic master equation approach developed in.[2–6]

3. CONCLUSIONS

Although the experimental situation on freeways is rather complex, we believe that some general features of traffic flow exist which can be described by relatively simple models. Dynamical models for car cluster formation based on stochastic methods (Master equation, Langevin equation, Fokker–Planck equation) have not been extensively exploited so far in traffic theory. It was the aim of the present contribution to present a stochastic description of jam formation using master equation approach. The main and central point is to construct the transition probabilities for the jump processes to condensate one free car to a car cluster or to evaporate the first congested car into free flow. This method allows us to interpret the phase transitions between different states of traffic flow in analogy to aggregation phenomena in metastable and unstable systems like supersaturated van der Waals gases.

ACKNOWLEDGMENTS

The authors gratefully acknowledges funding by German Science Foundation (DFG), grant MA 1508/6 (R. Mahnke), Graduiertenkolleg GK 567 and Academic International Office (J. Tolmacheva) as well as financial support by German Academic Exchange Program (DAAD) for J. Kaupužs and I. Lubashevsky.
The authors are indebted to R. Remer (Rostock), P. Wagner (Berlin) and H. Weber (Luleå) for fruitful discussions and support.

REFERENCES

1. J. Schmelzer, G. Röpke, and R. Mahnke, *Aggregation Phenomena in Complex Systems*, Wiley–VCH, Weinheim, 1999.
2. R. Mahnke, and N. Pieret, Stochastic master-equation approach to aggregation in freeway traffic, *Phys. Rev.* E **56**, 2666–2671, 1997.
3. R. Mahnke, and J. Kaupužs, Stochastic theory of freeway traffic, *Phys. Rev.* E **59**, 117–125, 1999.
4. R. Mahnke, and J. Kaupužs, Probabilistic description of traffic flow, *Networks and Spatial Economics* **1**, 103–136, 2001.
5. R. Mahnke, J. Kaupužs, and V. Frishfelds, Nucleation in physical and nonphysical systems, *Atmospheric Research* **65**, 261–284, 2003.
6. R. Mahnke, R. Kühne, J. Kaupužs, I. Lubashevsky, and R. Remer, Stochastic description of traffic breakdown, In: *Noise in Complex Systems and Stochastic Dynamics*, L. Schimansky–Geier, D. Abbott, A. Neiman, Ch. Van den Broeck, eds., Proc. SPIE **5114**, pp. 126–135, 2003.
7. R. Kühne, R. Mahnke, I. Lubashevsky, and J. Kaupužs, Probabilistic description of traffic breakdowns, *Phys. Rev.* E **65**, 066125, 2002.
8. M. Bando, K. Hasebe, A. Nakayama, A. Shibata, and Y. Sugiyama, Structure stability of congestion in traffic dynamics, *Japan J. Indust. and Appl. Math.* **11**, 203–223, 1994.
9. M. Bando, K. Hasebe, A. Nakayama, A. Shibata, and Y. Sugiyama, Dynamical model of traffic congestion and numerical simulation, *Phys. Rev.* E **51**, 1035–1042, 1995.
10. M. Bando, K. Hasebe, K. Nakanishi, A. Nakayama, A. Shibata, and Y. Sugiyama, Phenomenological study of dynamical model of traffic flow, *J. Phys. I France* **5**, 1389–1399, 1995.
11. F. R. Gantmacher, *Matrix Theory*, Nauka, Moscow, 1967; Dt. Verlag der Wiss., Berlin, 1986.
12. J. Kaupužs, H. Weber, J. Tolmacheva, and R. Mahnke, Applications to traffic breakdown on highways, In: *Progress in Industrial Mathematics at ECMI 2002*, A. Buikis, R. Ciegis, A. D. Fitt, eds., pp. 133–138, Springer, Berlin, 2004.
13. D. Helbing, Traffic and related self-driven many-particle systems, *Rev. Mod. Phys.*, **73**, 1067–1141, 2001.
14. P. E. Kloeden, E. Platen, *Numerical Solution of Stochastic Differential Equations*, Springer, Berlin, 1992.
15. D. Jost, K. Nagel, Probabilistic traffic flow breakdown in stochastic car following models, to be published in *Traffic and Granuar Flow (TGF) '03*.